Preprints of the 19th World Congress
The International Federation of Automatic Control
Cape Town, South Africa. August 24-29, 2014

Switching Fractional-Order Controllers of Common Rail Pressure in Compressed Natural Gas Engines ⋆

Paolo Lino * **Guido Maione** *

* *Dept. of Electrical and Information Eng., Politecnico di Bari, Bari, I-70125 Italy (e-mail: lino@deemail.poliba.it, gmaione@poliba.it)*

Abstract: This paper concerns fuel injection control of compressed natural gas engines. The main operating conditions are considered and for each one a fractional-order PI controller is designed. Then at each sudden change of rail pressure and injection timing, a change of the determined controller gains is scheduled. Switching between controllers is driven by step changes of the reference pressure. Robust stability of the designed closed-loop system is guaranteed by D-decomposition. Detailed simulation verifies both dynamic performance and robustness given by the controllers and stability of the switching.

1. INTRODUCTION

Over the past 20 years, Compressed Natural Gas (CNG) engines have experienced significant growth due to the environmental policy placing strict limits to the pollutants emission. However, it is not easy to achieve reduced pollutants emission. Only an accurate fuel metering, indeed, can form a stoichiometric air/fuel mixture. In CNG injection systems, proper fuel metering needs a precise control of both the gas injection pressure and the injection timings. Now, electronic control allows a precise adjustment of injectors opening time interval, whereas injection pressure regulation is difficult because the gas compressibility produces strongly nonlinear behavior. Basically, the variation of the working point, according to the power and speed requirements, and load disturbances or parametric variations of the environment make it difficult to precisely control the injection pressure.

Usually, the Electronic Control Units (ECUs) of vehicles implement PI controllers for regulating the injection pressure. These controllers are tuned once and for all as final solution, by applying heuristic rules, e.g. Ziegler-Nichols rules [2]. Typically, to take into account variations in the engine working condition, the gains of PI controllers are scheduled. Clearly, this solution does not guarantee optimal performance owing to nonlinearities, load disturbances, and plant parameters variations.

Therefore, to contribute to the researches on pressure control, this paper proposes a novel strategy combining fractional-order control with a scheduling technique. Noninteger or fractional-order proportional-integral-derivative (FOPID) controllers [27], also named fractional-order controllers (FOC) [3], are chosen because they have recently shown higher robustness than conventional PID controllers in many automotive applications, e.g. in car suspensions control [25]. The main feature of FOC is that they consider algorithms to approximate integration or differentiation of noninteger order. In particular, for each equilibrium point, a fractional-order proportional-integral (FOPI) controller is used to overcome the ordinary performance and robustness of PI controllers. This controller leads to good robustness and improves tuning flexibility because the fractional order of integration introduces a further degree-of-freedom in the design process.

Moreover, since a switching from an operating point to another is sometimes required, a scheduling strategy is adopted based on a sensitivity analysis of model parameters. Simulation is used to test performance and robustness and to show stability in switching [8]. Recent techniques based on LPV exist [22]. Here a different approach is followed to simplify the analysis and design.

The paper is structured as follows. Section 2 synthetically describes the injection model and its linearization. Section 3 explains the control strategy to cope with different equilibrium conditions. Sections 4 and 5 illustrate the design of FOPI controllers and how robust stability is obtained. Finally, Section 6 reports some simulation results for real operating conditions and Section 7 concludes the paper.

2. MODELING THE CNG INJECTION SYSTEM

The typical CNG injection system has the following main components: a fuel tank, a pressure reducer, a solenoid valve, a fuel metering system consisting of a common rail volume and electro-injectors, and an ECU (see Fig. 1 and [11] for more details). The tank stores high pressure gas and feeds the rest of the system. The mechanical pressure reducer includes a main chamber and a control chamber. A solenoid valve regulates the fuel entering the control chamber, the pressure of which actuates a second shutter for delivering the fuel in the main chamber. This chamber and a common rail are connected and share almost the same pressure. Then, the rail pressure is controlled by varying the duty cycle of the current that drives the solenoid valve. Note that the PWM modulation may cause oscillations, as the rail pressure increases (decreases) when

⋆ This work was supported in part by the Italian Ministry of University and Research under project *"EURO6 - Advanced electronic control unit, injection system, combustion strategies, sensors and production process technologies for low polluting diesel engines"*.

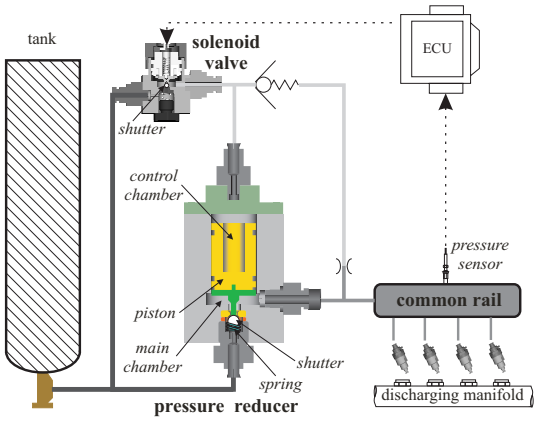

Fig. 1. The CNG injection system

the solenoid valve is open (closed) within the control period. However, efficiently controlling the rail pressure allows to meter the injected fuel by contemporaneously setting the opening time intervals of electro-injectors.

A state-space non-linear model [11] describes the rail pressure dynamics, where the pressures of the control chamber and rail are state variables, the control signal to the solenoid valve is the input, and the fuel injection process is a disturbance. A linearization process leads to a set of models with parameters depending on the actual working points. More in details, if a slowly varying then practically constant tank pressure is assumed, the ECU sets the injection pressure and timings and hence the actual working point. Moreover, the equilibrium values of the remaining variables are easily obtained from the nonlinear model [13], [14]. Under these assumptions, applying the Laplace transform to the linear model and neglecting the non-dominant dynamics yield a set of first order with time delay transfer functions [13], [14]

$$G_p(s) = \frac{K}{1+T\,s}\,e^{-\tau s} \qquad (1)$$

where s is the complex variable, the input and the output of $G(s)$ are the solenoid valve driving signal and the rail pressure, respectively. The parameters K, T, τ are, respectively, the static gain, the time constant of the dominant dynamics, and the dead time of the injection system, and each of them depends on the actual working point. At each equilibrium point, a different controller is tuned and then a scheduling policy schedules the controller gains switching from one working condition to another.

3. CONTROL STRATEGY

The new idea is to combine the potentialities of robust FOPI controllers with a scheduling strategy, as it is usually made by combining standard integer order PI controllers with a scheduling policy [30], [4]. Scheduling the controller parameters takes into account the different CNG engine working conditions for fuel injection, i.e. different equilibrium points. To each point corresponds a different controller that is designed according the approach of section 5. Choosing the appropriate controller for each working condition improves performance and robustness with respect to commonly used control strategies. Namely, for all operating conditions, injection systems usually employ only one simple PI controller that applies the conventional Ziegler-Nichols tuning rules [31, 5], [2], [11].

The scheduling strategy is synthetically the following. For each tank pressure, the working point is established by the rail pressure and by the average duration, say $\overline{I}$, of the injection process.Then, the rail pressure and $\overline{I}$ of the new required working point are taken as reference, and the variation from the current point to the required one is considered. Then, the FOPI controllers are tuned with reference to the set (K, T, τ) of parameters associated to the new equilibrium point. This always occurs when variations between a pair of operating points are bounded by 2 bar for the rail pressure and by 6 s for $\overline{I}$, respectively. However, if the variations are higher, then several intermediate pressure reference values (or $\overline{I}$ values) can be considered. Then, several sets of parameters are determined and several corresponding controllers are required. In this way, maps of controller gains are built for the different equilibrium points. This kind of strategy is common in many automotive applications [4], [23].

Two scheduling variables, i.e. the pressure reference and $\overline{I}$, are subject to step variations, to take the system to new equilibrium points. Since each local linear controller guarantees stability in the neighbors of corresponding equilibrium point, the step amplitudes have to be limited, in order to ensure that the initial state is in the region of attraction of the new equilibrium point [8]. Then, a smooth transition is achieved between equilibrium points.

In case of fast variations of scheduling variables, it is not possible to assess global stability for classical gain scheduling. Then stability in switching controllers is evaluated by simulation in Section 6 [28]. Recent design approaches, such as LPV [22], explicitly take into account time dependency of scheduling variables, so that global closed loop stability is *a priori* achieved [23]. The number and variation rate of scheduling parameters, as well as complexity of the nonlinear model, make the LPV framework not appropriate. Namely, analysis and design are complex, and the computational effort is high [23].

4. STABILITY ANALYSIS BY D-DECOMPOSITION

In control design the closed-loop stability is the first requirement. Then, this section builds the entire set of the controller gains leading to a stable closed-loop system. The motivation is twofold. First, consider the changes in working conditions during the injection control. Knowing the set of the gains can avoid time-consuming stability checks for any new controller settings and makes the tuning faster. Moreover, if the chosen controller gains correspond to a point of the set that is far from its boundary, then the stability is still ensured for (small) bounded variations of the controller gains. For this analysis, the D-decomposition methodology is useful [24]. This approach is well-established for the design of IO controllers in the parameter space [1], and has been also recently applied to investigate stability of control systems in which FOPID controllers operate on fractional order systems with delays [6], [15] , [7]. The effect of delays has been also investigated for designing classical PID controllers stabilizing fractional order systems [26]. The D-decomposition can determine all stabilizing FOPID controllers for integer or noninteger

order plants also when the plant transfer function is not known but its frequency response is at disposal [9].

This paper follows the procedure of [6], [15]. Consider the open-loop transfer function determined by the plant (1) and by a FOPI controller

$$G(s) = \frac{K\,K_I\,(1+T_I s^\nu)}{(1+Ts)\,s^\nu}\,e^{-\tau s}. \tag{2}$$

Then the closed-loop transfer function is

$$F(s) = \frac{K\,K_I\,(1+T_I s^\nu)\,e^{-\tau s}}{(1+Ts)\,s^\nu + K\,K_I\,(1+T_I s^\nu)\,e^{-\tau s}} \tag{3}$$

where ν is the fractional order of integration, $T_I = K_P/K_I$, and K_P and K_I are the proportional and integral gain, respectively. The roots of the fractional order characteristic pseudo-polynomial equation

$$E(s) = (1+Ts)\,s^\nu + K\,K_I\,(1+T_I s^\nu)\,e^{-\tau s} = 0 \tag{4}$$

determine stability of the control system: if all roots lie in the open left-half of the s-plane (LHP), i.e. no roots are in the closed right-half of the s-plane (RHP), then the closed-loop system is BIBO stable.

Then the set of all stabilizing controllers is determined by a complete stability region, say $\mathcal{D}$, in the parameter space associated to the triple (K_P, K_I, ν). Hence, if $(K_P, K_I, \nu) \in \mathcal{D}$ then all roots of (4) lie in the LHP. The stability domain $\mathcal{D}$ is defined by the so-called real root boundary (RRB), the infinite root boundary (IRB), and the complex root boundary (CRB) [6], [1]. The RRB is associated to $s = 0$, then to the solutions of $E(s = 0) = 0$:

$$K\,K_I = 0 \Rightarrow K_I = 0 \tag{5}$$

The CRB comes from $E(s = j\omega) = 0$

$$\begin{aligned}&(1+Tj\omega)\,\omega^\nu\,(C+jS)+\\&+K\,K_I\,[1+T_I\omega^\nu(C+jS)]\,[\cos(x)-j\sin(x)] = 0\end{aligned} \tag{6}$$

with $C = \cos(\theta), S = \sin(\theta), \theta = \frac{\pi}{2}\nu, x = \omega\tau$. Taking the real and imaginary parts of the complex equation (6) leads to the following solutions:

$$\begin{aligned}K_I(\omega) &= \frac{\omega^\nu\,(\sin(x)+\omega T\cos(x))}{K\,S}\\ T_I(\omega) &= \frac{(\omega TS - C)\,\sin(x) - (S+\omega TC)\,\cos(x)}{\omega^\nu\,(\sin(x)+\omega T\cos(x))}\\ K_P(\omega) &= \frac{(\omega TS - C)\,\sin(x) - (S+\omega TC)\,\cos(x)}{K\,S}\end{aligned} \tag{7}$$

that can be used to plot a curve in a 2D-space (K_P, K_I) (or (K_P, T_I) or (T_I, K_I)), when ν is fixed and ω is varied from 0 to ∞. The IRB for $s \to \infty$ does not exist [6].

Now, in a first step, one of the parameters is fixed so that the stability regions and their boundaries belong to the plane defined by the remaining two parameters. In a second step, the fixed parameter is varied and the complete 3D stability domain is obtained by sweeping over all the admissible values of this parameter. For example, if ν is fixed, then the boundaries specified by RRB and CRB divide the parameter plane (K_P, K_I) into unstable and stable regions, that can be distinguished by checking one arbitrary test point within each region. Algorithms for checking stability were given by [7] and [21].

In the CNG injection system, τ is approximately constant. Namely, $\tau = 0.05$ seconds in the whole operating range of an accurate model of a real CNG engine, see Section 6. Moreover, representative working conditions are considered according to the values of the rail pressure, p_r, and injection timing, t_{inj}, and an engine speed of 2500 rpm, thereby providing different pairs (K, T) of the system parameter values (see Table 1). Then one can design a different FOPI controller for each operating point and obtain a different stability domain for each pair (K, T) (see Fig. 2 for a specific working point). In particular, instead of showing the complete 3D stability domain, Fig. 2 plots its projections on the plane (K_P, K_I), i.e. the stability region, for $\nu = 1.3, 1.4, 1.5, 1.6$. The values of the gains are indicated but a multiplying factor of 10^{-2}. Similar plots could limit stability regions in the planes (K_P, T_I) or (T_I, K_I), but they are omitted here for sake of space.

Table 1. Engine parameters in working points

p_r (bar)	t_{inj} (ms)	K (bar)	T (s)
4	5	165	1.74
6	5	136	1.71
8	5	118	1.95
10	5	127	1.97

The stability regions are delimited by the CRB curves (solid lines) and by the horizontal RRB line. All CRB curves start from $(K_P, K_I) = (-1/K, 0)$, for $\omega = 0$ rad/second, and cross the RRB line at the same point. Note that, for a given value of ν, the point (marked with $\times$ in Fig. 2) is associated to the designed values of K_P and K_I inside the stability region. Moreover, this point belongs to a "relative stability curve" obtained by considering the specified phase margin PM_s and using the technique of the phase margin tester [6], [15]. More in details, this further line is obtained by increasing the pure dead-time in $G(s)$ by PM_s. Then, in (7), x is replaced by $y = x + PM_s$, where PM_s is the stability margin. Each point in the line corresponds to a frequency. In this case, the relative stability line starts from $(K_P, K_I) = (-1/(K\,S), 0)$, for $\omega = 0$ rad/second. Obviously, the point determined by the designed gains corresponds to the specified gain crossover frequency, ω_c. Finally, the distance between the CRB curves and the design points, i.e. the associated relative stability lines, gives a measure of the robustness level.

A similar line of reasoning can be followed to define a relative stability line associated to a gain margin GM_s (not shown in Fig. 2). This curve can be determined by amplifying $G(s)$ by GM_s, then by replacing K by $K\,GM_s$ in (7). Again, each point on the curve corresponds to a frequency, and the designed controller gains determine a point associated to the phase crossover frequency.

5. DESIGN PROCEDURE

For each operating point, a FOPI controller is designed by applying a loop-shaping approach [12]. In the proposed methodology, relatively easy closed formulas directly relate performance and robustness specifications to the values of the controller gains. An integrator of noninteger order ν, $1 < \nu < 2$, achieves robustness to gain variations by leading to an open-loop frequency response (OLFR for short) with a nearly flat phase diagram and a constant slope of the magnitude diagram in a sufficiently wide frequency range around the crossover [12]. Moreover, the optimality of the feedback system is pursued by shaping

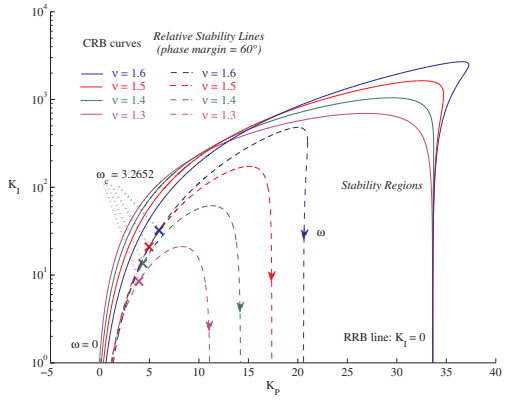

Fig. 2. Stability regions, relative stability lines, and controllers designed for the first working point ($u_c = 5.7$)

the OLFR so that its gain is high at low frequencies and rolls off at high frequencies [29]. In this way, a good input-output tracking is obtained in a specified bandwidth.

Consider a unitary feedback control system, in which sensor dynamics are neglected for simplicity, and with the plant model (1). Let the FOPI controller use a standard proportional action and an integral action of noninteger order $1 < \nu < 2$:

$$G_c(s) = K_P + \frac{K_I}{s^\nu} = \frac{K_I}{s^\nu}\,(1 + T_I\, s^\nu) \tag{8}$$

with $T_I = \frac{K_P}{K_I}$ and where K_P and K_I are the proportional and integral gain, respectively. Therefore, an increased flexibility is due to three design parameters (i.e. one more degree of freedom with respect to a PI controller). However, a reliable and effective design rule must be established. Putting $s = j\omega$ yields the OLFR associated to $G(s) = G_c(s)\,G_p(s)$, that is

$$G(j\omega) = \frac{K\,K_I\,[1 + T_I\,(j\omega)^\nu]}{(j\omega)^\nu\,(1 + j\omega\,T)}\,e^{-j\omega\tau}. \tag{9}$$

Now, after introducing $u = \omega T$, using S and C as previously defined allows to simply obtain

$$G(ju) = \frac{K\,K_I\,T^\nu\,\left\{1 + T_I\,(\frac{u}{T})^\nu\,[C + jS]\right\}}{u^\nu\,[C + jS]\,(1 + j\,u)}\,e^{-j\,\frac{u\tau}{T}} \tag{10}$$

with

$$\begin{aligned} |G(ju)| &= \frac{K\,K_I\,T^\nu}{u^\nu}\,\sqrt{\frac{1 + 2\,T_I\,(\frac{u}{T})^\nu\,C + T_I^2\,(\frac{u}{T})^{2\nu}}{1 + u^2}} \\ \angle G(ju) &= \arctan\left(\frac{T_I\,(\frac{u}{T})^\nu\,S}{1 + T_I\,(\frac{u}{T})^\nu\,C}\right) - \arctan(u) - \theta - \frac{u\tau}{T} \end{aligned} \tag{11}$$

Now, the requirement $|F(ju)| \equiv 1$ is approximated in a significant bandwidth u_B, where $F(ju) = \frac{1}{1+G^{-1}(ju)}$ is the closed-loop frequency response. In theory, however, an optimal feedback system should be achieved only if this holds true for all frequencies, i.e. $|G(ju)| \gg 1, \forall u$. Instead, $|G(ju)|$ is shaped around the crossover u_c to guarantee robust stability and desired performance despite parameter variations in the controlled injection system.

To synthesize, the first step chooses u_B where optimal tracking is requested. In particular, a trade-off is reached between high values reducing the rise time in the system closed-loop response, and lower values shifting u_c (which is itself a measure of the bandwidth) toward the center of the flat region of the phase characteristic. For sake of convenience, u_B is chosen higher than the plant bandwidth.

The normalized crossover is estimated by $u_c \in [\frac{u_B}{1.7}, \frac{u_B}{1.3}]$, e.g. $u_c = \frac{u_B}{1.5}$. (Changing the estimate and playing inside this range allows us to adjust T_I.) Then, to achieve a specified phase margin PM_s at u_c, T_I is properly selected. Namely, if the phase margin $PM = \pi + \angle G(ju_c)$ is:

$$\begin{aligned} PM = &\arctan\left(\frac{T_I\,(\frac{u_c}{T})^\nu\,\sin(\theta)}{1 + T_I\,(\frac{u_c}{T})^\nu\,\cos(\theta)}\right) - \arctan(u_c) - \frac{u_c\tau}{T} \\ &+ \pi - \theta = \varphi_1(u_c) - \varphi_2(u_c) - \frac{u_c\tau}{T} + \pi - \theta \end{aligned} \tag{12}$$

where $\varphi_1(u_c)$ and $\varphi_2(u_c)$ are the first two arguments on the right side of (12). Then, T_I is chosen to compensate the delay by $\varphi_1(u_c) - \varphi_2(u_c) - u_c\,\frac{\tau}{T} = 0$ and to obtain a closed formula:

$$T_I = \frac{T^\nu\,[u_c + \tan(\frac{u_c\tau}{T})]}{u_c^\nu\,[S - u_c\,C - (C + u_c\,S)\,\tan(\frac{u_c\tau}{T})]}. \tag{13}$$

This choice yields:

$$PM_s = \pi - \theta = (2 - \nu)\,\pi/2 \Leftrightarrow \nu = 2 - 2PM_s/\pi \tag{14}$$

that represents a direct and easy design relation between the fractional order ν and PM_s. Note that (14) gives $\nu > 1$ for a plant without integrator. Obviously, at the end of the design procedure, it is always verified that the FOPI controller leads to a nearly flat Bode plot of $\angle G(ju)$ with a nearly constant phase margin in a wide range around u_c.

The condition $|G^{-1}(ju_c)|^2 = 1$ leads to another closed formula for determining K_I:

$$K_I = \frac{1}{K}\,\left(\frac{u_c}{T}\right)^\nu\,\sqrt{\frac{1 + u_c^2}{1 + 2\,T_I\,(\frac{u_c}{T})^\nu\,C + T_I^2\,(\frac{u_c}{T})^{2\nu}}}. \tag{15}$$

The (15) also leads to $K_P = K_I\,T_I$.

Now, the approximation of the irrational operator s^ν by a rational transfer function completes the design procedure. An efficient approach employs continued fraction expansions [17] and *a priori* guarantees interlacing [19] between negative real minimum-phase zeros and stable poles of the approximation. Closed formulas express coefficients of numerator and denominator of the transfer function and avoid numerical problems [19]. Interlacing can be enforced also for digital realization [16], [18], [20]. Moreover, the number of required zeros and poles to obtain a reduced approximation error is relatively low, so that an easy implementation is possible.

The previously described design procedure determines the points marked by $\times$ in Fig. 2. The controller gains correspond to nominal values of (K, T, τ). One can verify that changing the fractional order ν varies the shape of the stability region, but it does not affect the closed-loop stability, while preserving the same specifications on the phase margin and on the crossover frequency. Moreover, the points are quite far from the CRB of the stability region, thereby ensuring a good level of robustness.

As regards the obtained performance, one may choose larger u_c to increase u_B and then the promptness of response. Hence one can move the design point along the relative stability line in the sense of increasing frequencies, to augment or diminish the integral and proportional actions. Following the line, however, the same phase margin PM_s

Table 2. Values of T_I with $\nu = 1.5$ for different pairs (r, u_c), and with different ν for a working condition with $r = 0.0286$ and for $u_c = 5.7$

(r, u_c)	T_I (s)
$(0.8, 5.0294)$	1.5897
$(0.8, 5.7000)$	-0.1225
$(0.8, 6.5769)$	0.0573
$(1.0, 5.0294)$	0.0313
$(1.0, 5.7000)$	0.1233
$(1.0, 6.5769)$	0.2259
$(1.2, 5.0294)$	0.1959
$(1.2, 5.7000)$	0.4015
$(1.2, 6.5769)$	-0.0246

ν	PM	T_I (s)	τ_{max} (s)
1.1	81°	1.6320	0.1013
1.2	72°	0.7579	0.1494
1.3	63°	0.4635	0.1975
1.4	54°	0.3200	0.2456
1.5	45°	0.2372	0.2937
1.6	36°	0.1847	0.3418
1.7	27°	0.1493	0.3899
1.8	18°	0.1245	0.4381
1.9	9°	0.1067	-0.4760

is kept. A good position could be the point of maximum of K_I, on the top of the relative stability line. This position can be obtained by an optimization procedure.

Remark 1. The absolute value and sign of T_I depend on the choice of ν (i.e. PM_s) and u_c (i.e. u_B). Then, if u_c is fixed, ν is restricted to allow $T_I > 0$. Viceversa, if ν is fixed, the same restriction applies on u_c. For example, for $\nu = 1.5$, Table 2 provides the values of T_I for several pairs (r, u_c), where $r = \tau/T$ is the delay ratio and $u_c \in \{u_B/1.7, u_B/1.5, u_B/1.3\}$, with $u_B = 8.55$. In particular, given T, u_c, and ν, the maximum plant delay allowing $T_I > 0$ is $\tau_{max} = \left(\frac{T}{u_c}\right) \arctan\left(\frac{S - u_c C}{C + u_c S}\right)$. Then, τ_{max} depends on plant parameters and specifications u_B and PM_s. Moreover, values $\nu \geq 1.6$ are not convenient because they imply a too low phase margin, which is usually taken greater than 35° [29]. Table 2 also shows the values of T_I for $u_c = u_B/1.5 = 5.7$, $\tau = 0.05$ seconds and $T = 1.74$ seconds ($r = 0.0286$) that hold for a particular injection working point (see Table 1 and section 6). In all cases, $\tau < \tau_{max}$. Then the controller design is possible.

6. SIMULATION ANALYSIS

In this section, a detailed model created by the AMESim developing package is the main tool for evaluating the performance of the controlled system. AMESim is a multi-domain virtual prototyping tool produced by IMAGINE S.A. It enables the modeling of components from different physical domains and their integration in an overall system framework [10]. It also guarantees a flexible architecture, capable of including new components defined by the users. The resulting model is highly nonlinear and properly describes the complex fluid dynamic phenomena characterizing the injection system at different working points. Hence the model is a virtual prototype, very similar to the actual hardware in providing an extremely reliable representation of the controlled system.

To test efficiency and robustness of the control, the FOPI controllers, with $\nu = 1.3, 1.4, 1.5, 1.6$, are compared to a PI controller that is typically used for injection control and tuned by the open-loop Ziegler-Nichols rules. Values of $\nu < 1.3$ are not considered because they lead to too high phase margins, neither are values of $\nu > 1.6$ because they provide too low phase margins, i.e. below 36°.

With reference to the typical working conditions in Table 1, two different cases are simulated. In the first case there is a small reference pressure variation from 4 to 5 bar. Moreover, the injection timing is 5 milliseconds, the engine speed is 2500 rpm, and the tank pressure is 50 bar. A single FOPI or PI controller is used with the (K, T) parameters associated to the final pressure.

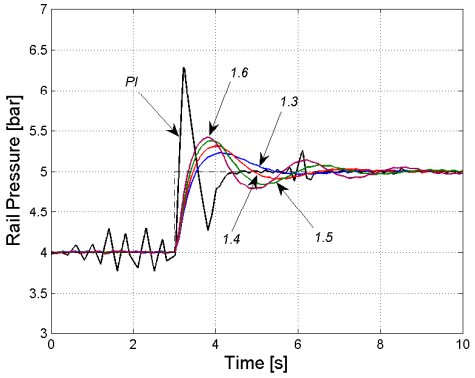

Fig. 3. Response to a 1 bar step of reference pressure

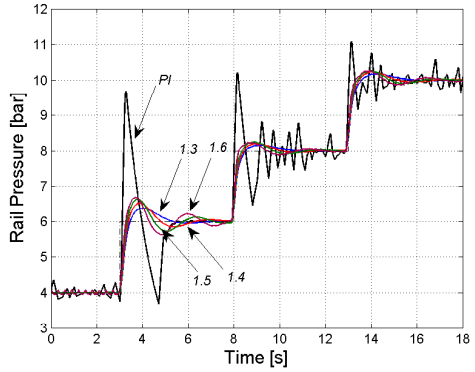

Fig. 4. Response to large variations of reference pressure

Fig. 3 shows the closed-loop step response. With respect to the standard PI controller, FOPI controllers improve the performance indices: even if the rise time is slightly longer, overshoot is highly reduced, then a better accuracy is achieved in injection; the settling times are comparable for $\nu \leq 1.5$. With the PI controller, the performance is influenced primarily by disturbances and nonlinearities related to injectors operations, by PWM modulation of the solenoid valve command, and by saturation of the actuator. In fact, large variations of the control signal cause high frequency pressure oscillations around the equilibrium point. Moreover, the saturation in the control signal, which is associated to a complete closure of the valve, determines large rail pressure overshoots and undershoots. Conversely, fractional controllers performances are less sensitive to system disturbances and nonlinearities.

The second case simulates a large variation in the reference pressure from 4 to 10 bar. Then, the scheduling switches between several controllers. In particular, the variation is divided in 3 steps, then 3 FOPI/PI controllers are used.

Fig. 4 shows that FOPI reduce the overshoot significantly and that responses are similar to the first case. Conversely, PI controller poorly reacts to larger variations, and the previously described nonlinear phenomena considerably affect overall performance. Therefore, FOPI may improve pressure regulation also for these large perturbations.

7. CONCLUSIONS

Usually, a unique PI controller for all working conditions controls injection in CNG engines. In this paper, a new control strategy conjugates the benefits of FOPI controllers with a proper scheduling of their gains. Pressure is regulated by tuning different FOPI controllers on the basis of the reference working points. A D-decomposition method guarantees the closed-loop robust stability for each working condition and FOPI controllers achieve higher robustness and dynamic performance, especially for large variations of reference pressure. As far as switching is concerned, simulation shows that choosing sufficiently close working points prevents stability problems.

REFERENCES

[1] J. Ackermann and D. Kaesbauer. Stable polyhedra in parameter space. *Automatica*, 39 (5), 937–943, 2003.

[2] C. Amorese, S. De Matthaeis, O. De Michele, and A. Satriano. The gaseous fuel option: LPG and CNG. In *Proc. Int. Conf. on Vehicles Alternative Fuel System & Envir. Protection*. Dublin, Ireland, July 6–9, 2004.

[3] Y.Q. Chen. Ubiquitous fractional order controls?. In *Proc. of the Second IFAC Symp. on Fractional Derivatives and its Applications*, vol. 2, 168–173. Porto, Portugal, July 19-21, 2006.

[4] A. di Gaeta, U. Montanaro, G. Fiengo, A. Palladino, and V. Giglio. A model-based gain scheduling approach for controlling the common-rail system for GDI engines. *Int. J. of Control*, 85 (4), 419-436, 2012.

[5] G. Fiengo, A. di Gaeta, A. Palladino, and V. Giglio. *Common Rail System for GDI Engines - Modelling, Identification, and Control*. Springer Briefs in Electrical and Computer Engin., Springer, London, 2013.

[6] S.E. Hamamci. An algorithm for stabilization of fractional-order time delay systems using fractional-order PID controllers. *IEEE Trans. Automatic Control*, 52 (10), 1964–1969, 2007.

[7] C. Hwang and Y.C. Cheng. A numerical algorithm for stability testing of fractional delay systems. *Automatica*, 42 (5), 825–831, 2006.

[8] H.K. Khalil. *Nonlinear Systems*, 3rd ed.. Prentice-Hall, Upper Saddle River, NJ, 2002.

[9] Y.K. Lee and J.M. Watkins. Determination of all stabilizing fractional-order PID controllers. In *Proc. 2011 Amer. Control Conf.*, 5007–5012. San Francisco (CA), USA, June 29 - July 01, 2011.

[10] P. Lino and B. Maione. Integrated design of a mechatronic system - The pressure control in common rails. In *Proc. 4th Int. Conf. Informat. in Control, Autom. and Robot.*, 11–18. Angers, France, May 9-12, 2007.

[11] P. Lino, B. Maione, and C. Amorese. Modelling and predictive control of a new injection system for compressed natural gas engines. *Control Engineering Practice*, 16 (10), 1216–1230, 2008.

[12] P. Lino and G. Maione. Loop-shaping and easy tuning of fractional-order proportional integral controllers for position servo systems. *Asian Journal of Control*, 15 (3), 796–805, May 2013.

[13] P. Lino and G. Maione. Fractional order control of the injection system in a CNG engine. In *2013 Europ. Contr. Conf.*, 3997–4002. Zürich, Switzerland, July 17-19, 2013.

[14] P. Lino and G. Maione. Design and simulation of fractional-order controllers of injection in CNG engines. In T. Kawabe (ed.), *7th IFAC Symp. Adv. Automot. Contr.*, 582–587. Tokyo, Japan, Sep. 4-7, 2013.

[15] Y. Luo, Y.Q. Chen. Stabilizing and robust fractional order PI controller synthesis for first order plus time delay systems. *Automatica*, 48 (9), 2159–2167, 2012.

[16] G. Maione. Concerning continued fractions representations of noninteger order digital differentiators. *IEEE Signal Proc. Lett.*, 13 (12), 725–728, Dec. 2006.

[17] G. Maione. Continued fractions approximation of the impulse response of fractional order dynamic systems. *IET Contr. Theory & Appl.*, 2 (7), 564–572, July 2008.

[18] G. Maione. High-speed digital realizations of fractional operators in delta domain. *IEEE Trans. Autom. Control*, 56 (3), 697–702, Mar. 2011.

[19] G. Maione. Conditions for a class of rational approximants of fractional differentiators/integrators to enjoy the interlacing property. In S. Bittanti, A. Cenedese, and S. Zampieri (eds.), *Proc. 18th IFAC World Congr.*, 13984–13989. Milan, Italy, 28 Aug. - 2 Sep. 2011.

[20] G. Maione. On the Laguerre rational approximation to fractional discrete derivative and integral operators. *IEEE Trans. Autom. Control*, 58 (6), 1579–1585, 2013.

[21] D. Matignon. Stability result on fractional differential equations with applications to control processing. In *Proc. of IMACS-IEEE SMC Conf.*, vol. 2, 963–968. Lille, France, July 9-12, 1996.

[22] M. Moze, J. Sabatier, A. Oustaloup. Air-fuel ratio control of an internal combustion engine using CRONE control extended to LPV systems. In D. Baleanu, Z.B. Güvenç, and J.A. Tenreiro Machado (Eds.), *New Trends in Nanotechnology and Fractional Calculus Applications*, 71–86. Springer, 2010.

[23] G.J.L. Naus. Model-based control for automotive applications. PhD Thesis, Technische Universiteit Eindhoven, http://dx.doi.org/10.6100/IR690571, 2010.

[24] Yu.I. Neimark. *Ustoichivost' linearizovannykh sistem upravleniya (Stability of Linearized Control Systems)*. LKVVIA, Leningrad, 1949.

[25] A. Oustaloup. *La Commande CRONE. Command Robuste d'Ordre Non Entièr*. Ed. Hermès, Paris, 1991.

[26] H. Özbay, C. Bonnet, and A.R. Fioravanti. PID controller design for fractional-order systems with time delays. *Syst. & Contr. Lett.*, 61 (1), 18–23, 2012.

[27] I. Podlubny. Fractional-order systems and $PI^{\lambda}D^{\mu}$-controllers. *IEEE Trans. Autom. Control*, 44 (1), 208-214, 1999.

[28] W.J. Rugh and J.S. Shamma. Research on gain scheduling. *Automatica*, 36 (10), 1401-1425, 2000.

[29] S. Skogestad and I. Postlethwaite. *Multivariable Feedback Control: Analysis and Design*, 2nd ed.. Wiley & Sons, Ltd., Chichester, England, 2005.

[30] Z. Sun and S.S. Ge. *Switched Linear Systems. Control and Design*. Springer Verlag, 2005.

[31] A.G. Ulsoy, H. Peng, and M. Çakmakci. *Automotive Control Systems*, 1st ed.. Cambridge University Press, Cambridge, 2012.